RERTR 2011 – 33rd INTERNATIONAL MEETING ON
REDUCED ENRICHMENT FOR RESEARCH AND TEST
REACTORS

October 23-27, 2011
Marriott Santiago Hotel
Santiago, Chile

Nanomechanical Behavior of U-10Mo/Zr/Al Fuel Assemblies

N.A. Mara
Materials Science and Technology Division and the Center for Integrated Nanotechnologies Los Alamos National Laboratory, MS-K771, Los Alamos, NM 97545 USA

J. Crapps, T. Wynn, K. Clarke, P. Dickerson, D.E Dombrowski, B. Mihaila
Materials Science and Technology Division Los Alamos National Laboratory
Los Alamos, NM 97545 USA

A. Antoniou Woodruff
School of Mechanical Engineering
Georgia Institute of Technology, Atlanta, GA 30332

ABSTRACT

We present the nanomechanical behavior of U-10Mo/Zr/Al fuel assemblies using nanoindentation and nanocantilever bend testing. In these assemblies, fracture is often observed near the interfaces between constituents, and may be attributed to microstructural features such as carbide inclusions, intermetallic phases, voids, etc. Nanoindentation testing gives hardness values for U-10Mo, Zr, and Aluminum in as-HIPed fuel assemblies (4.4 GPa, 2.2 GPa, and 1.2 GPa respectively). Nanocantilevers prepared via Focused Ion Beam (FIB) are tested in a nanoindenter. By scaling the yield strength of bulk material data while maintaining hardening behavior, load-displacement output from a finite element simulation of identical geometry is matched with load-displacement data from tests allowing correlation between local and higher level mechanical behavior. Our measurements show the effect of voids and chemical segregation on Al-Al HIP bonds, and the comparable strength of the U-10Mo/Zr interface with respect to Zr. Measured mechanical behavior will be discussed in terms of the influence of interfacial morphology, crystallography, and chemistry on strength and ductility of the interface.

1. Introduction

Recent research into U-10Mo/Zr/Al plate fuel assemblies, has illustrated the importance of fundamentally understanding interfacial mechanical behavior. The parameters and phenomena that have been noted include existence of stress gradients at interfaces and their influence on bond strength [1], and strength and fracture behavior of the various interfaces before and after irradiation [2]. Bend testing [3] and pull testing [4] have been used to gain some insight on the

mechanical behavior of the composite plate, but as noted in [5], neither method can isolate the mechanical behavior of a specific bond.

The plate geometry specifications [6, 7], include a U-10Mo layer 250 microns thick, a Zr interlayer is 30 microns thick and the Al cladding is 250 microns thick, the overall sample thickness is less than 1mm. As a result conventional macroscopic mechanical tests have had difficulty in gaining insight about the mechanical behavior of individual interfaces. In order to give local information about the deformability of the regions in the vicinity of the interface, in this work, nanomechanical test methodologies are employed, specifically nanoindentation and cantilever bend testing.

Several different methods have been used to test small volumes ($<\mu m^3$) of material, including micropillars [8, 9], and nanoindentation [10]. While these make up the majority of the growing data set of materials and geometries tested at the nanoscale, other methodologies such as tensile [11] and cantilever bend testing [12-16] have been utilized to a lesser extent to test material response under different stress states, particularly tensile stresses. Microcantilever testing provides a tensile stress state over part of the sample, and offers relatively straightforward sample manufacturing, as well as the capability to perform the test ex-situ in a commercial nanoindenter without the need of a Scanning Electron Microscope (SEM) to provide proper alignment between grips and sample. In this work, we utilize the microcantilever technique to investigate the mechanical behavior of Al-6061/Al-6061, U-10Mo/Zr, and Zr/Al interfaces produced via Hot Isostatic Pressing (HIP). [17] Cantilevers of nominally 5 micron by 5 micron cross section and 20 micron length are produced via FIB machining and deformed using conventional nanoindentation techniques. This methodology gives load-displacement data, which, in the case of the Al/Al bond, is then analyzed via Finite Element Modeling (FEM) to determine the yield strength of the cantilever containing the bond. While microcantilevers have been used before to investigate fracture and mechanical response of systems based on tightly controlled thin film deposition techniques [12, 13, 15, 16], this work focuses on the robustness of this technique in determining the local effects of interfacial chemistry and voids on bond strength of nuclear fuel assemblies.

2. Experimental Set-up

The experimental setup is similar to that found in Mara et al. [18] The bonded plates examined here were fabricated based on a hot isostatic press (HIP) process to bond 6061-aluminum cladding to U-10 wt pct Mo fuel foils (with co-rolled Zr diffusion barrier), nominally using the methodologies described by Jue, et al[17]. However, in the case of the Al-Al bond the process was scaled-up to produce 61 cm x 7.6 cm fuel plate assemblies and the HIP cycle consisted of a 120 minute hold at 560°C and 138 MPa. The Zr/U-10Mo and Zr/Al interfaces followed the Jue et al. procedure. Samples for this study were taken from several regions: 1.) A region where only the two 3.8 cm aluminum plates are in contact and are HIP bonded under the above conditions, 2.) In the Al material away from the HIP bond, 3.) Material containing the Al-Zr interface, and 4.) Material containing the U-10Mo/Zr interface.

Microcantilevers were FIB machined to include the above interfaces and constituent materials. The bonded interface was incorporated normal to the long axis of the microcantilevers, approximately 3-5 μ m from the base, in order to subject it to tensile stresses. The microcantilevers for this study were manufactured using a FEI Helios NanoLab 600 Dual Beam SEM/FIB operating at 30 keV. The cantilevers were cut to a pentagonal cross section as used in previous fracture studies[14], so that cracks would initially propagate with constant width. The

cantilevers had an average width of 5 μm, thickness of 5 μm, and length of 20 μm. Each cantilever was first cut to a rough shape using a 21 nA gallium ion beam. The initial step was to mill a "U" shaped trench into the bulk of the sample, then tilt the sample 45 degrees and undercut from each side. Final cantilever shape was milled with a 0.92 nA ion beam to clean and shape each side of the cantilever, and to remove any redeposited material. After milling, each

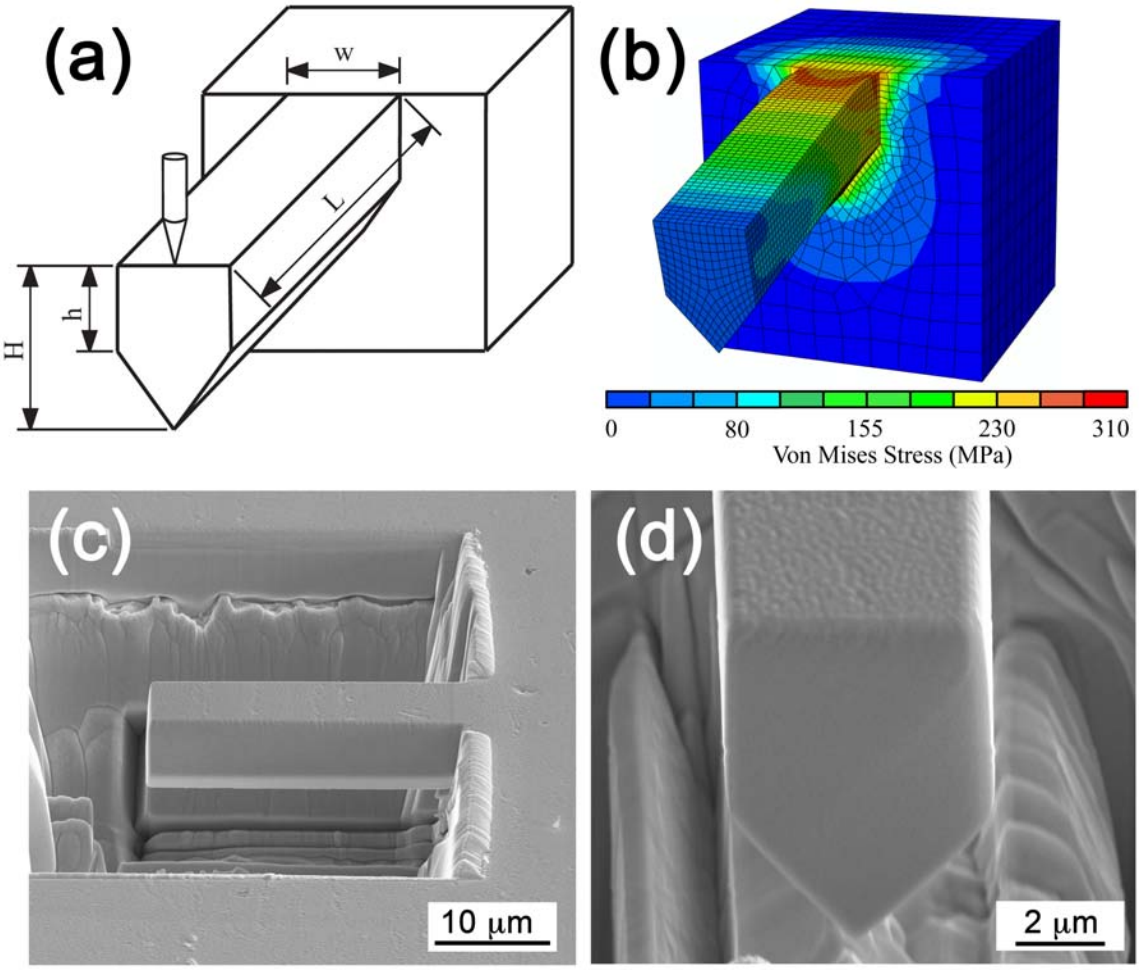

cantilever was imaged using an SEM before testing to allow the actual width and thickness to be measured.

Figure 1: (a) Schematic of microcantilever beam geometry. **(b)** FEM model of cantilever after undergoing plastic deformation showing mesh and stress distribution over the cantilever. **(c)** SEM micrograph of an as-FIB prepared microcantilever. **(d)** end view of the microcantilever seen in (c). [18]

Once the cantilevers were fabricated, they were tested using commercially available nanoindenters (Hysitron Triboindenter 900, Agilent nanoXP) fitted with Berkovich tips, where load and displacement data were acquired as a function of time. Quasistatic displacement rates of typically ~67 nm/second were chosen. The cantilevers were deformed 5 microns from the cantilever end. The cantilever, with loading geometry as shown in Figure 1, was then examined via SEM after deformation to ensure that plastic deformation was most prevalent at the cantilever hinge, and to locate the exact point of loading. The compliance associated with the indentation mark left in the end of the cantilever was subtracted from the overall displacement by using indentation data from the bulk of the material.

Finite-element (FE) simulations were used to understand the cantilever deformation experiments and infer the mechanical properties of HIP-ed Al and Al-Al interfaces at the sub-micron scale. Simulations were performed using the commercially available finite-element platform ABAQUS. Mesh refinement studies of the model illustrated schematically in Fig.1a and Fig. 1b were carried out to assure that all numerical results presented here were converged with respect to the mesh size.

3. Results

Nanoindentation testing with a Berkovich tip was carried out to a depth of 300 nm on each of the three constituent phases: Al, Zr, and U-10Mo in order to determine their relative strengths. From these tests, the strength and reduced modulus values as seen in Table 1 were obtained. The elastic modulus values for U-10Mo and Zr are in reasonable agreement with those found elsewhere [19], but the Al is a bit higher than that for pure Al, which is 68 GPa. These slightly elevated values for modulus and hardness can be attributed to excessive pile up around indents in soft metals as noted in [20].

Material	Avg E (GPa)	SD E (GPa)	Avg H (GPa)	SD H (GPa)
U-10Mo	107.3	5.5	4.4	0.3
Zr	106.3	6.3	2.2	0.1
Al	83.0	4.6	1.2	0.1

Table 1: Hardness and reduced modulus values for the constituent materials

From these relative hardness values, it was determined that to test the Al/Zr bond, Al would be the base of the cantilever to ensure that local deformation near the indenter would not dominate the test, and in the case of U-10Mo/Zr interfaces, that Zr would constitute the base of the cantilever.

3.1 Al and Al-Al HIP Bonds

Utilizing an FEM model that incorporates the work hardening rate from bulk as-HIPed 6061-Al, and a Young's Modulus of 68 GPa, it was found that the response of an as-HIPed Al cantilever with no visible grain boundaries could be accurately described by simply increasing the yield strength to account for the increased strength associated with deforming small volumes (up to 10's of cubic microns) of material. [18] In Figure 2, this model is applied to an as-HIPed

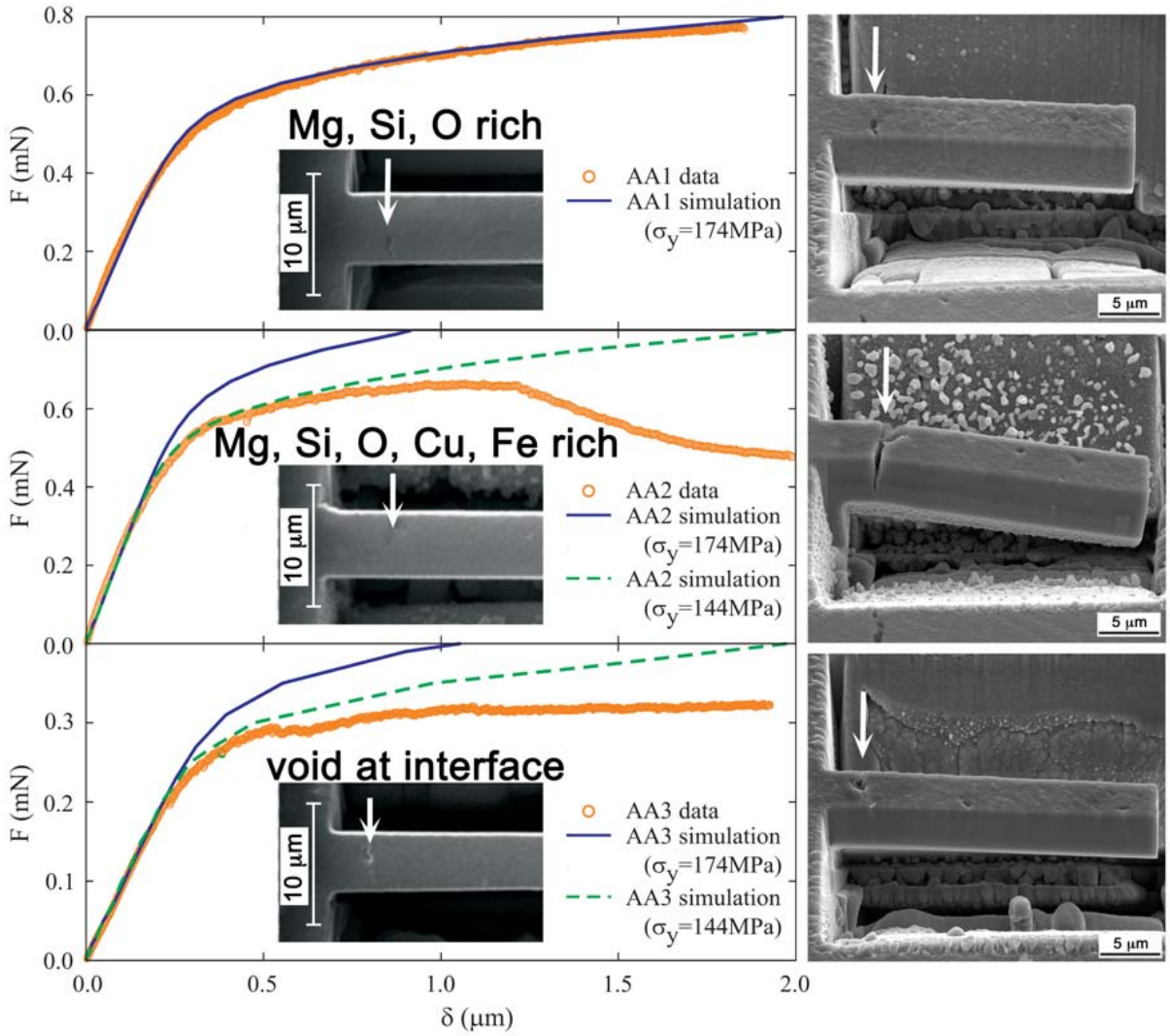

Al-Al interface, with the load-displacement curve and as-machined cantilever for the test on the left accompanied by the corresponding as-deformed cantilever on the right. It is seen that for an interface rich in Mg, Si, and O (Figure 2, top panel), as verified by Energy Dispersive Spectroscopy (not shown) that the material behaves similarly to the monolithic Al cantilever mentioned above, σy = 174 MPa, and constitutes a high quality bond with no observable cracking at the interface. The FEM model matches the entire load-displacement data well in

Figure 2: Load-displacement curves for three different Al-Al interfaces, with interface location noted by arrows. The top figure is of a cantilever with minimal chemical segregation to the interface, and exhibits behavior similar to the interface-free cantilever of similar size shown in

Fig.2. The center and lower figures show the load-displacement behavior for cantilevers containing large inclusions and voids, respectively. For good agreement between the model and experiment in the two latter cases, yield strength of the material had to be reduced by 17%. [18]

However, when a large Mg, Si, O, Cu, Fe rich precipitate is located at the Al-Al boundary (Figure 2, center panel), behavior differs from the ideal case. Deformation is localized to the interface, where fracture is evident, and in order to have agreement between FEM and experimental data, the yield strength of the cantilever must be decreased by 17% (dashed green line). Remarkably, the elastic modulus and work hardening rates do not need to be altered—good agreement up to fracture at 1.25 microns displacement depends only on changing the yield stress. The effect of a 2 micron diameter void is seen in Figure 2, bottom panel, where a similar drop in yield stress is required to provide good agreement between FEM and experiment (dashed green line).

In this study, we showed that FE simulations could successfully assist in the quantitative understanding of the small-scale material properties of HIP-ed Al as determined by microcantilever testing. The results of our FE simulations indicate that at small loads the cantilevers deform elastically with the same elastic modulus as in bulk. The onset of plasticity occurs at yield stress values with a strong volumetric effect. The mechanical performance of the cantilever remains unchanged in the absence of inclusions or pores at the bonded interfaces. Interfaces with different chemistry (inclusions) lead to a reduction in the yield stress and these cantilevers fail at moderate loading. The onset of plastic behavior in cantilevers with missing mass (voids) at the grain interfaces occurs at reduced values of the yield stress as in the case of

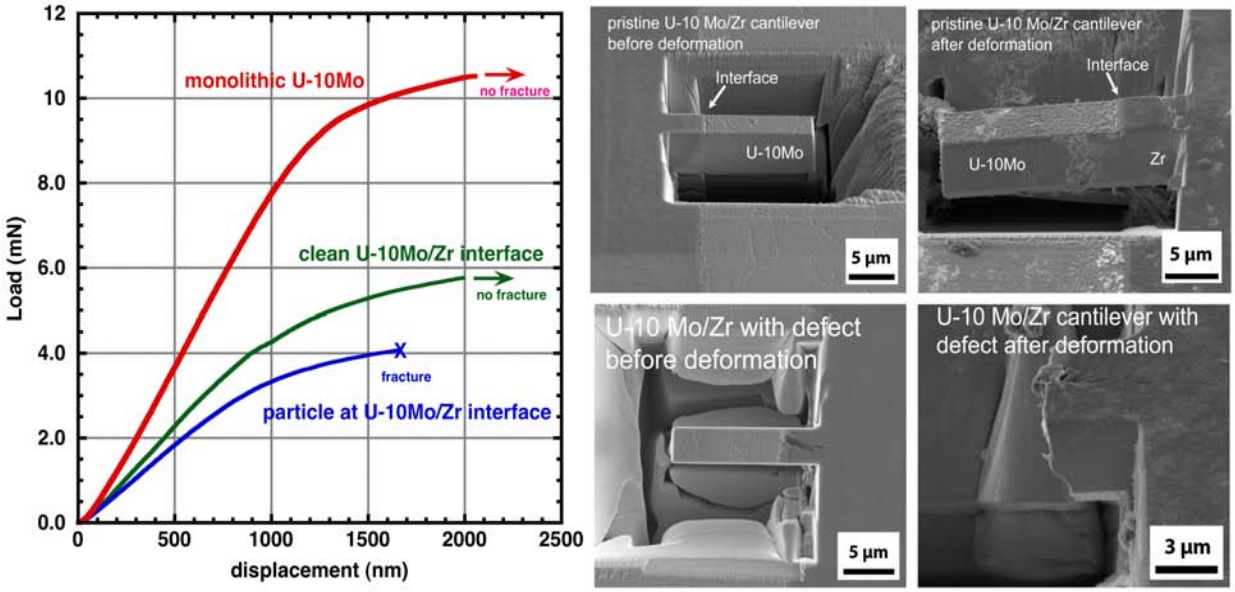

inclusions at the interface, but these cantilevers become more compliant at modest subsequent displacement increases.

Figure 3: Load vs. Displacement curves for monolithic U-10Mo and cantilevers with U10Mo/Zr interface before and after testing. In all pristine U-10Mo/Zr cantilevers, deformation was localized in the Zr phase as seen in the top two SEM micrographs. The two lower SEM micrographs show fracture localized at the interface due to the presence of an inclusion.

The load-displacement behavior of monolithic (no discernible interfaces near the cantilever hinge) U-10Mo, "pristine" U-10Mo/Zr, and U-10Mo/Zr interfaces containing a zirconia inclusion are shown in Figure 3, with the before and after deformation SEM micrographs of interface-containing samples seen to the right.

The monolithic U-10Mo deformed in a controlled fashion without fracture after 2 microns displacement, and so the SEM micrographs are not shown. A minimum of 3 pristine interfaces were tested, with all localized yielding occurring in the Zr phase and no fracture evident at the interface. However, when an inclusion is located at the U-10Mo/Zr interface, fracture is localized at that interface.

3.3 Zr/Al bonds

Figure 4 shows the typical (minimum of 3 tests) load-displacement and fracture behavior of an as-HIPed Zr/Al interface. In contrast to the U-10Mo/Zr interface, fracture is always located at the Al/AlZr interaction layer interface, and plasticity in the Al is evident despite large inclusions

Figure 4: Cantilevers with Zr/Al interface before and after testing. Note the localized plastic

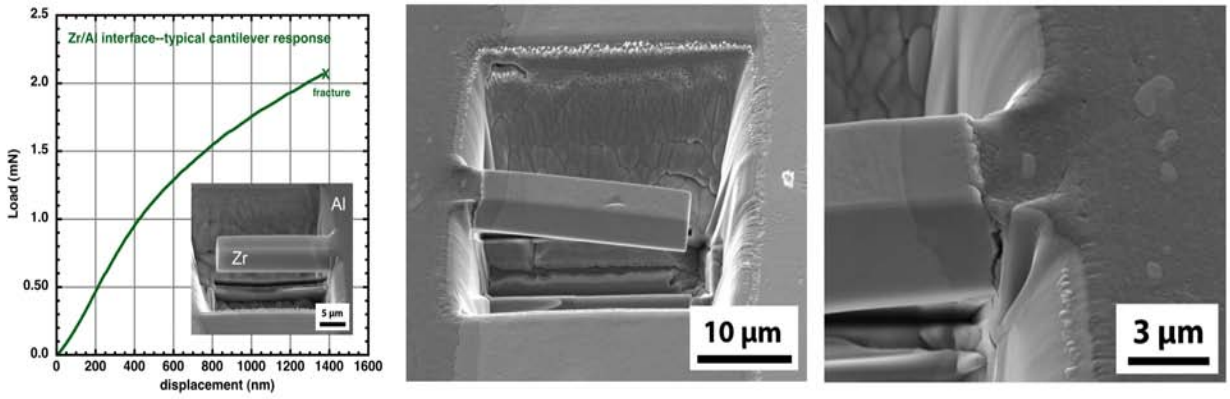

deformation in the Al base of the cantilever, and fracture at the interface between the Al and AlZr reaction layer.

4. Discussion

In this work, the microcantilever bend test has elucidated some of the local mechanical behavior of interfaces in U-10Mo/Zr/Al fuel assemblies. Due to the constraints of the fuel plate geometry, to date, no other technique has given quantitative or qualitative data about the individual interfaces between the constituent materials in any systematic way. However, as with any micro or nano scale test, there are several issues that must be addressed such that the interpretation of such tests can be as meaningful as possible. These are:

1.) Volumetric effects: strengthening due to a dislocation starved microstructure
2.) Effect of grain orientation
3.) Effect of testing single grain versus polycrystalline samples
4.) Moment (Torque) magnitude effect

Volumetric effects: As was revealed by the tests of pure Al cantilevers with no discernible boundaries [18], there is a "smaller is stronger" size effect in these cantilevers. That is, the cantilever bend test measured a yield strength of 174 MPa, whereas the bulk yield strength as measured by a tension test was 44 MPa. This type of size effect has been seen in micropillar compression tests where the pillar diameter was on the order of the cantilever width used here [8]. The strengthening effect has been attributed to dislocation starvation, where there are not enough sources of defects to give a yield strength consistent with a "bulk" response, and so higher stresses are needed to operate less ideal dislocation sources with an associated energy penalty. However, if the distribution of these sources is homogeneous throughout the sample, and the cantilever size is kept constant, direct comparisons between different interfaces can be made. With the constraints made by fuel plate geometries where the Zr interlayer is only a few tens of microns thick, measurement of interfacial mechanical behavior without any size effects will be difficult at best.

Grain orientation effects: Given the constituents of the fuel plate: bcc U-10Mo, fcc Al, and hcp Zr, only Zr is highly anisotropic in its elastic and plastic behaviors. Since the size of the cantilever is close to the grain size of the material, some anisotropy, and therefore grain orientation effects could be expected in Zr. This remains to be studied. However, in Al, our FEM model was able to accurately represent the cantilever bend test without inputting any grain orientation information, and points to grain orientation effects in highly symmetric fcc materials as playing a secondary role. We are currently investigating monolithic U-10Mo cantilever bend tests to determine if this can be applied to bcc materials as well.

Effects of single grain deformation vs. polycrystalline deformation: Some of these effects are tied closely to the grain orientation effect discussed in #2 above. With highly isotropic materials, this effect will be lessened. However, we have shown that the strength of a given interface is limited by the distribution and type of inhomogeneities found at that interface. That being said, microcantilever testing of regions free from such inhomogeneities can give an upper bound estimate for the strength of the interface, and can locally probe which inhomogeneities are critical to bond strength. We found that the chemical segregation of Mg, Si, and O to the Al-Al HIP bond was not necessarily deleterious to the strength of the bond. Only once these start to form particles of ~2 micron diameter do they begin to affect bond strength. Clearly, a more polycrystalline representation of the interface could be useful in terms of understanding macroscopic fracture of the interface. These experiments are planned in the near future, and will utilize larger cantilevers as the fuel plate geometry will allow.

Moment (Torque) magnitude effects: The accuracy to which the indenter tip can be placed on the end of the cantilever is an important consideration in defining loading geometry. In this case, all cantilevers are examined in the SEM after testing, making such quantities known within a few 10's of nanometers. Furthermore, the effects of moving the actuation point across the width of the cantilever were evaluated in the FEM model, and had little effect on the stress at which the cantilever yielded. However, in the case of gross misalignment where the indenter is nearly off of the cantilever, the elastic modulus deviates significantly from the correct value, and so provides a built-in method of determining which data points are valid. In all of the data presented here, the location of the indent was deemed sufficient as to minimize these moment (torque) effects.

With the above points in mind, the cantilever bend test data can be interpreted to give strength values in the case of Al and Al-Al HIP bonds, and bond strength of the U-10Mo/Zr and Zr/Al bonds relative to the strength of the constituents. For the Al-Al HIP bonds, it was found that a

17% decrease in yield strength results when inclusions or voids of diameter ~2 micron are present at the Al-Al boundary. This quantitative result, while still exhibiting a volumetric strengthening effect, does allow for an understanding of critical flaw size, and how it relates to bond strength.

While the load-displacement data still needs to be analyzed via FEM to give numeric strength values at the site of fracture, some information can be gleaned from the fracture behavior of U-10Mo/Zr and Zr/Al bonds. In the U-10Mo/Zr system, it was found that the interface was always as strong as the Zr constituent, provided that there is no segregation of large particles to the boundary. In the case of Zr-Al, fracture is somewhat more complicated, with significant plasticity in the Al parent material, followed by localized fracture along the Al/AlZr interaction layer boundary. Future work is planned to investigate this interface further to determine the exact composition and phase of the material where fracture occurs.

5. Conclusions

This study into the nanomechanical behavior of U-10Mo/Zr/Al fuel plates yields the following conclusions:

1.) By measuring the strength of the constituent U-10Mo, Zr, and Al phases separately via nanoindentation, it was found that their relative strengths, as expected, decrease in that order.

2.) FE simulations successfully assist in the quantitative understanding of the small-scale material properties of HIP-ed Al and Al-Al bonds as determined by microcantilever testing. The results of our FE simulations indicate that at small loads the cantilevers deform elastically with the same elastic modulus as in bulk. The onset of plasticity occurs at yield stress values with a strong volumetric effect. The hardening behavior of HIP-ed Al is largely the same as that of bulk Al.

3.) In the case of Al-Al and U-10Mo/Zr bonds, the mechanical performance of the cantilever containing an interface remains as strong as the weakest constituent in the absence of inclusions or pores at the bonded interfaces. Interfaces with different chemistry (inclusions) lead to a reduction in the yield stress and these cantilevers fail at moderate loading localized at the site of the defect. The bulk elastic characteristics of the linear part of the force *vs* displacement curves in both loading and unloading regimes provide a reliable test for eliminating flawed experimental data.

4.) In the case of Zr/Al bonds, the fracture behavior is more complicated than that found in U-10Mo/Zr or Al/Al bonds, and consists of localized yielding of the Al phase and fracture occurs along the boundary between the Zr/Al interaction layer and the Al phase.

5.) Given the above, we conclude that the strength of the constituents/interfaces are in the following order from strongest to weakest: U-10Mo≥U-10Mo/Zr>Zr>Zr/Al≈Al. Quantification of the strengths of each interface will require additional FE models, which are currently under development.

6. Acknowledgements

The authors would like to acknowledge the financial support of the US Department of Energy Global Threat Reduction Initiative Reactor Convert program. This work was performed, in part, at the Center for Integrated Nanotechnologies, a U.S. Department of Energy, Office of Basic Energy Sciences user facility. Los Alamos National Laboratory, an affirmative action equal opportunity employer, is operated by Los Alamos National Security, LLC, for the National Nuclear Security Administration of the U.S. Department of Energy under contract DE-AC52-06NA25396.

7. References

[1] H. Ozaltun, P.G. Medvedev, in: RRFM 2010: 14. international topical meeting on Research Reactor Fuel Management (RRFM), Marrakech (Morocco), 21-25 Mar 2010; , pp. 11.

[2] A.B. Robinson, G.S. Chang, D.D. Keiser, D.M. Wachs, D.L. Porter, in, Idaho National Laboratory, 2009.

[3] J.M. Wight, G.A. Moore, S.C. Taylor, in: RERTR 2008 International Meeting on Reduced Enrichment for Research and Test Reactors,Hamilton Crowne Plaza Hotel in Washington D.C.,10/05/2008,10/09/2008, United States, 2008.

[4] D.D. Keiser, J.F. Jue, D.E. Burkes, in: 11th International topical meeting. Research Reactor Fuel Management (RRFM) and meeting of the International Group on Reactor Research (IGORR), Lyon (France), 11-15 Mar 2007; , France, 2007, pp. 111-117.

[5] D.E. Burkes, D.D. Keiser, D.M. Wachs, J.S. Larson, M.D. Chapple, in: 11th International topical meeting. Research Reactor Fuel Management (RRFM) and meeting of the International Group on Reactor Research (IGORR), Lyon (France), 11-15 Mar 2007; , France, 2007, pp. 426-430.

[6] G.A. Moore, B.H. Rabin, J.F. Jue, C.R. Clark, N.E. Woolstenhulme, B.H. Park, S.E. Steffler, M.D. Chapple, M.C. Marshall, J.J. Green, B.L. Mackowiak, in: RERTR 2010, Lisbon, Portugal, 2010.

[7] J. Katz, K. Clarke, B. Mihaila, J. Crapps, B. Aikin, V. Vargas, R. Weinberg, in: RERTR 2011, Santiago, Chile, 2011.

[8] J.R. Greer, J.T.M. De Hosson, Progress in Materials Science, 56 (2011) 654-724.

[9] M.D. Uchic, D.M. Dimiduk, J.N. Florando, W.D. Nix, Science, 305 (2004) 986-989.

[10] W.C. Oliver, G.M. Pharr, MRS Bulletin, 35 897-907.

[11] J.-Y. Kim, J.R. Greer, Acta Materialia, 57 (2009) 5245-5253.

[12] D.E.J. Armstrong, A.J. Wilkinson, S.G. Roberts, Philosophical Magazine Letters, 91, 394-400.

[13] D.E.J. Armstrong, A.J. Wilkinson, S.G. Roberts, Journal of Materials Research, 24 (2009) 3268-3276.

[14] D. Di Maio, S.G. Roberts, Journal of Materials Research, 20 (2005) 299-302.

[15] K. Matoy, T. Detzel, Mu, uml, M. ller, C. Motz, G. Dehm, Surface & Coatings Technology, 204 (2009) 878-881.

[16] K. Matoy, H. Schoànherr, T. Detzel, T. Schoàberl, R. Pippan, C. Motz, G. Dehm, Thin Solid Films, 518 (2009) 247-256.

[17] J.-F. Jue, B.H. Park, C.R. Clark, G.A. Moore, D.D. Keiser Jr, Nuclear Technology, 172 204-210. N.A. Mara, J. Crapps, T. Wynn, K. Clarke, A. Antoniou, P. Dickerson, D.E. Dombrowski, Mihaila, Submitted to: Scripta Materialia, (2011).

[19] D.O. Northwood, I.M. London, L.E. Bahen, Journal of Nuclear Materials, 55 (1975) 299-310.

[20] T.Y. Tsui, W.C. Oliver, G.M. Pharr, in: Thin Films: Stresses and Mechanical Properties VI. Symposium ; 8-12 April 1996 ; San Francisco, CA, USA, Mater. Res. Soc, Pittsburgh, PA, USA, pp. 207-212.